



Published in final edited form as:

Cell Rep. 2018 April 10; 23(2): 596–607. doi:10.1016/j.celrep.2018.03.045.

Genome-wide CRISPR/Cas9 Screen Identifies Host Factors Essential for Influenza Virus Replication

Julianna Han^{1,5}, Jasmine T. Perez^{1,5}, Cindy Chen¹, Yan Li², Asiel Benitez³, Matheswaran Kandasamy¹, Yoontae Lee⁴, Jorge Andrade², Benjamin tenOever³, and Balaji Manicassamy^{1,6,*}

¹Department of Microbiology, The University of Chicago, Chicago, IL 60637, USA

²Center for Research Informatics, The University of Chicago, Chicago, IL 60637, USA

³Department of Microbiology, Icahn School of Medicine at Mount Sinai, New York, NY 10029, USA

⁴Department of Life Sciences, Pohang University of Science and Technology, Pohang, Kyungbuk 790-784, Republic of Korea

SUMMARY

The emergence of influenza A viruses (IAVs) from zoonotic reservoirs poses a great threat to human health. As seasonal vaccines are ineffective against zoonotic strains, and newly transmitted viruses can quickly acquire drug resistance, there remains a need for host-directed therapeutics against IAVs. Here, we performed a genome-scale CRISPR/Cas9 knockout screen in human lung epithelial cells with a human isolate of an avian H5N1 strain. Several genes involved in sialic acid biosynthesis and related glycosylation pathways were highly enriched post-H5N1 selection, including *SLC35A1*, a sialic acid transporter essential for IAV receptor expression and thus viral entry. Importantly, we have identified capicua (*CIC*) as a negative regulator of cell-intrinsic immunity, as loss of *CIC* resulted in heightened antiviral responses and restricted replication of multiple viruses. Therefore, our study demonstrates that the CRISPR/Cas9 system can be utilized for the discovery of host factors critical for the replication of intracellular pathogens.

In Brief

This is an open access article under the CC BY-NC-ND license (<http://creativecommons.org/licenses/by-nc-nd/4.0/>).

*Correspondence: bmanicassamy@bsd.uchicago.edu.

⁵These authors contributed equally

⁶Lead Contact

DATA AND SOFTWARE AVAILABILITY

The accession number for the deep sequencing data reported in this study is GEO: GSE111166.

SUPPLEMENTAL INFORMATION

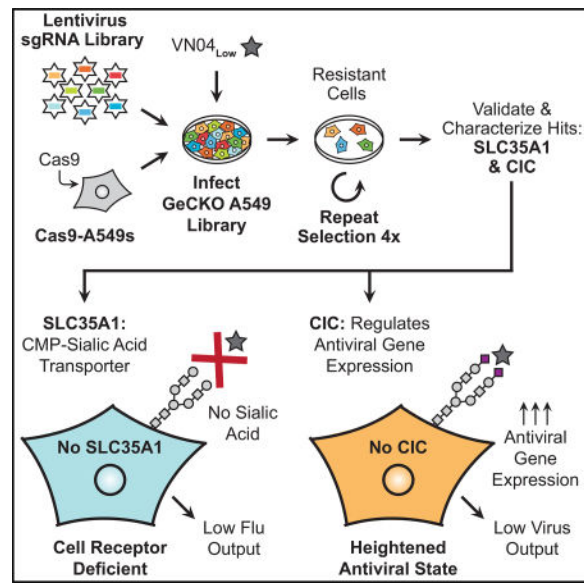
Supplemental Information includes Supplemental Experimental Procedures, five figures, and seven tables and can be found with this article online at <https://doi.org/10.1016/j.celrep.2018.03.045>.

AUTHOR CONTRIBUTIONS

J.H., J.T.P., and B.M. conceived and designed the study. A.B. and B.t. performed Illumina sequencing. Y. Li and J.A. analyzed the sgRNA distribution. J.H., J.T.P., C.C., M.K., and B.M. performed the experiments. Y. Lee provided the *CIC* and the ATXN1L antibodies. J.H., J.T.P., and B.M. wrote the manuscript. All authors approved the manuscript.

DECLARATION OF INTERESTS

The authors declare no competing interests.



Using a genome-wide CRISPR/Cas9 screen, Han et al. demonstrate that the major hit, the sialic acid transporter SLC35A1, is an essential host factor for IAV entry. In addition, they identify the DNA-binding transcriptional repressor CIC as a negative regulator of cell-intrinsic immunity.

INTRODUCTION

Influenza A virus (IAV) is an upper respiratory pathogen in humans with the ability to rapidly evolve, resulting in both seasonal epidemics and occasional pandemics (Wright et al., 2013). As the constant emergence of variant- and drug-resistant strains greatly reduce the efficacy of current vaccines and therapies, there remains a need for host-directed therapeutics against IAVs. Multiple genome-wide screening approaches, including small interfering RNA (siRNA), proteomic, and insertional mutagenesis screens, have been employed to identify host factors involved in IAV infection (Hao et al., 2008; Brass et al., 2009; Karlas et al., 2010; König et al., 2010; Ward et al., 2012; Su et al., 2013; Benitez et al., 2015; Shapira et al., 2009; Sui et al., 2009; Watanabe et al., 2014). Although some common hits and pathways were revealed, most notably members of the vacuolar ATPase family, meta-analyses demonstrated little overlap in the identified IAV host factors, likely because of differences in the strains used, time points assayed, and functional readouts chosen (Mehle and Doudna, 2010; Stertz and Shaw, 2011; Watanabe et al., 2010). Therefore, alternative screening strategies will provide the flexibility needed to uncover host factors and pathways, as well as validate previously identified hits, to serve as potential targets for the development of anti-influenza therapeutics.

Recent advancements in CRISPR/Cas9 technology have allowed for gene disruption on a genome-wide scale in mammalian cells (Shalem et al., 2014; Wang et al., 2014; Wright et al., 2016). Recently, the GeCKO (genome-wide CRISPR knockout) screening strategy has been utilized to investigate virus-host interactions (Haga et al., 2016; Ma et al., 2015; Marceau et al., 2016; Orchard et al., 2016; Park et al., 2017a; Savidis et al., 2016; Zhang et al., 2016). Here, we generated a GeCKO library in human lung epithelial (A549) cells

negatively selected against genes essential for cell viability and subjected this A549-GeCKO library to five rounds of lethal infection with a human isolate of an avian IAV strain. Deep sequencing analysis of the enriched single guide RNA (sgRNA) population identified numerous genes involved in the sialic acid biosynthesis and glycosylation pathways, as well as in the regulation of cell-intrinsic immunity. Validation studies revealed host factors critical for multiple IAV strains that function at different stages of viral replication, including entry and antiviral responses. Loss of *SLC35A1*, a CMP-sialic acid transporter, rendered cells resistant to IAV infection because of the absence of cell-surface sialic acids. Furthermore, GeCKO screening identified capicua (*CIC*), a DNA-binding transcriptional repressor, as a negative regulator of cell-intrinsic immunity. Loss of *CIC* resulted in upregulation of antiviral responses and restricted replication of viruses from diverse families. Taken together, our studies demonstrate that GeCKO screening is a versatile strategy that can be utilized to identify host factors critical for IAV replication.

RESULTS

Generation of an A549-GeCKO Library

To identify host genes critical for IAV replication, we generated a GeCKO library in A549 cells as previously described and performed a genome-scale loss-of-function genetic screen (Shalem et al., 2014; Wang et al., 2014; Zhang et al., 2016). First, we derived a clonal Cas9-expressing A549 cell line (Cas9-A549s) by transducing wild-type (WT) A549 cells with lentivirus expressing the Cas9 gene (Figure 1A, step 1). Next, Cas9-A549s were transduced with lentivirus containing a pooled human genome-wide sgRNA library (library A) of 65,383 sgRNAs targeting 19,050 protein-coding genes and 1,864 microRNA (miRNA) precursors and selected in puromycin for 14 days (Figure 1A, steps 2–4) (Sanjana et al., 2014; Shalem et al., 2014). To evaluate sgRNA diversity in the A549-GeCKO library, we PCR-amplified the integrated sgRNA cassettes from genomic DNA and subjected them to Illumina sequencing. Analysis of the 9M reads obtained from 1×10^8 cells revealed the presence of 62,659 sgRNAs (> 10 reads) in the A549-GeCKO library, representing an average coverage of $\sim 140\times$ per sgRNA (Figures S1A and S1B). The loss of $\sim 4.2\%$ of sgRNAs post-puromycin selection likely suggests the negative selection of a non-viable cell population. Thus, we successfully generated a pooled GeCKO library in A549 cells with sufficient coverage to perform genetic screens for IAV host factors.

Preliminary Screen for Positive Selection of H5N1-Resistant Cells in the A549-GeCKO Library

To enrich for a cell population resistant to IAV replication, we subjected the A549-GeCKO library to lethal infection with a human isolate of a low pathogenic avian H5N1 virus (A/Vietnam/1203/04, VN04_{Low}; Figure 1A, steps 5–7). For our preliminary GeCKO screen, we performed five consecutive rounds (Rd) of lethal infection with minimal expansion of cells between rounds (preliminary consecutive screen); the resistant cells were subsequently expanded, and sgRNA distribution was assessed by Illumina sequencing (Prelim Rd5; Figure 1A, steps 8a–9). For the 8M Illumina reads obtained from Prelim Rd5, we observed robust enrichment of 586 sgRNAs (> 10 reads) representing $\sim 1\%$ of the sgRNAs present in the A549-GeCKO library (Figures S1A and S1C). Next, candidate genes were identified and

ranked using the model-based analysis of genome-wide CRISPR/Cas9 knockout (MAGeCK) program (Li et al., 2014). We observed positive selection of 119 genes in Prelim Rd5 ($p < 0.1$), with the *SLC35A1* gene (sialic acid transporter) ranked highest and demonstrating representation by all 3 independent sgRNAs (Table S1). Interestingly, the remaining genes showed enrichment for a single sgRNA, likely because of the stringent selection achieved by performing five consecutive rounds of lethal infection with minimal expansion of cells between rounds. Together, our preliminary screen identified potential host factors whose loss rendered cells highly resistant to H5N1 infection.

Analysis of sgRNA Enrichment during Sequential H5N1 Selection

Next, we performed a less stringent GeCKO screen by allowing for substantial expansion of surviving cells between each round of H5N1 selection (sequential screen; Figure 1A, steps 8b–9). This would allow us to determine if progressive enrichment of sgRNAs occurs at each round of selection, such that genes critical for H5N1 replication are represented by multiple sgRNAs in the earlier rounds. We assessed sgRNA representation at each round of infection in duplicate sample sets up to five rounds. Comparative analysis of sgRNA representation between the A549-GeCKO library and Rd1 of the sequential screen showed no significant differences (Figures 1B and S1A). In contrast, we observed robust enrichment of specific sgRNAs at Rd2, with a progressive increase in enrichment occurring between Rd2–5. These data indicate that selection of a cell population less permissive to H5N1 occurs after two rounds of lethal infection.

Next, we performed principle component analysis (PCA) and Pearson correlation analysis to understand the sgRNA distribution pattern between biological replicates in the sequential screen. The sgRNA distribution profile of Replicate one (Rep1, red) and Replicate two (Rep2, blue) at Rd1 clustered together and remained close to the A549-GeCKO library; however, in subsequent rounds (Rd2 to Rd5), the samples belonging to each replicate closely clustered within their respective groups, indicating divergence of replicates after Rd2 (Figure S1D). Similarly, comparison of individual sample sets showed strong correlation of sgRNA distribution between Rep1 and Rep2 at Rd1, with a correlation coefficient value of 0.92; however, the correlation coefficient value decreased to 0.25 in subsequent rounds (Figure S1E). Although replicate divergence occurred at Rd2, we observed enrichment of specific sgRNAs common in both replicates (Table S1). Taken together, these results demonstrate that the robust enrichment seen at Rd2 of the sequential screen occurred concurrently with replicate divergence, yet revealed the progressive enrichment of a common sgRNA population between replicates.

Identification of Genes Enriched during Sequential H5N1 Selection

Next, we performed MAGeCK analysis to identify positively selected genes at Rd2 and Rd5 of the sequential screen (Table S1). We observed enrichment of 798 genes ($p < 0.05$) at Rd2, with 161 genes represented by two or more sgRNAs and 637 genes represented by a single sgRNA (Figure 1C). However, we observed enrichment of 501 genes ($p < 0.05$) at Rd5, with only 16 genes represented by two or more sgRNAs, and 485 genes represented by a single sgRNA. This decrease in the number of genes represented by multiple sgRNAs between Rd2 and Rd5 suggests that stringent H5N1 selection results in the preferential enrichment of

individual sgRNAs. To further evaluate the genes identified at Rd5, we compared our hits to factors identified in the nine previously reported genome-wide screens for influenza virus (Brass et al., 2009; Hao et al., 2008; Karlas et al., 2010; König et al., 2010; Su et al., 2013; Ward et al., 2012; Shapira et al., 2009; Sui et al., 2009; Watanabe et al., 2014). Comparative analyses of the hits identified at Rd5 ($p < 0.05$), excluding miRNAs, indicated that 33 of the 453 hits were also identified in previous screens (Figure 1D; Table S2). Vacuolar ATPase family members, which were highly represented in six of the prior screens, were also highly enriched in the sequential screen (*ATP6API1*, *ATP6AP2*, *ATP6V0A1*, *ATP6V0B*, *ATP6V0C*, *ATP6V1B2*, *ATP6V1G1*, and *ATP6V1H*) (Mehle and Doudna, 2010; Stertz and Shaw, 2011; Watanabe et al., 2010). In addition, we identified >400 unique genes, demonstrating that GeCKO screening can reveal previously unidentified IAV host factors.

Next, we used the R package for reactome pathway analysis to identify enriched biological processes and determined that 117 genes from Rd2 and 133 genes from Rd5 ($p < 0.05$) mapped to known biological processes (Figure 1E; Table S3) (Yu and He, 2016). We observed enrichment for genes involved in proton transport and vacuolar acidification, which were represented in the prior genome-wide screens for influenza virus (Figure 1D; Table S2). We also observed enrichment for genes involved in sialic acid biosynthesis, protein glycan modification, and glycosylphosphatidylinositol (GPI)-anchor synthesis, as well as genes involved in intracellular signaling pathways, regulation of cell-intrinsic immunity, and autophagy. Therefore, the GeCKO screening confirmed previously described processes, such as vacuolar acidification, and highlighted other processes, including sialic acid biosynthesis and glycan modification, that are important for IAV replication.

Confirmation of Top Hits via Individual Gene KO

To prioritize the candidate host factors for further validation, we identified the common genes in the sequential (Rd5) versus consecutive (Prelim Rd5) screens (Figure 2A; Table S4). Of the 63 genes in common, we selected 11 highly enriched candidates representing various biological processes for the generation of individual CRISPR KO cell lines (Table 1). Eight hits (*SLC35A1*, *GDF11*, *IRX3*, *C2CD4C*, *TRIM23*, *PIGN*, *ACADSB*, and *GRAMD2*) were also highly enriched ($p < 0.05$) in the early rounds of selection (Rd2), and the remaining three hits (*CIC*, *JAK2*, and *PIAS3*) demonstrated enrichment only after multiple rounds of selection (Figure S2). To determine if these candidate genes are important for IAV replication, the 11 generated polyclonal KOs were infected with H5N1 at a low multiplicity of infection (MOI). A >60% reduction in viral titer was observed in eight KOs as compared to vector control cells, demonstrating that GeCKO screening was successful in identifying H5N1 host factors in A549 cells (Figure 2B).

As we anticipated incomplete disruption of target gene loci in the polyclonal population, we next generated seven clonal KOs for a subset of host factors. Sequence analysis of the sgRNA target sites in the clonal KOs indicated that complete gene disruption was achieved in all but the *CIC* KOs, which contained a WT allele (Table S5). We evaluated H5N1 replication in the clonal KOs, and observed an ~5 log reduction in viral titer in *SLC35A1* and *CIC* KOs, as well as a >80% reduction in viral titer in the remaining KOs as compared to vector control cells (Figure 2C). The robust reduction in H5N1 titer observed in the clonal

KOs as compared to their respective polyclonal populations suggests that complete gene disruption was required for the validation of candidate host factors. To exclude the possibility of off-target effects in the clonal KOs, we analyzed the sgRNA sequences for potential complementarity in the exons of the human genome (Table S6). A minimum of 3–4 mismatches were required for identification of potential off-target genes, the majority of which were not enriched at Rd2 and Rd5 of the sequential screen ($p < 0.05$). As the seven evaluated clonal KOs demonstrated robust reduction in H5N1 viral titer and limited potential for off-target effects, we have thus confirmed that these hits are important for H5N1 replication.

Validation of Hits with Multiple IAV Strains

To determine if the validated host factors are required for the replication of multiple IAV strains, we infected the clonal KOs with H1N1 (A/Puerto Rico/8/1934; PR8) and H3N2 (A/Hong Kong/1/1968; HK68) at a low MOI. We observed a >5 log reduction in viral titer in *SLC35A1* KOs and a >3 log reduction in viral titer in *CIC* KOs as compared to vector control cells (Figure 2C). Interestingly, *PIAS3* KOs demonstrated strain specificity, as a $>80\%$ reduction in viral titer was observed for H1N1 and H5N1, yet H3N2 replication was unaffected. The remaining clonal KOs showed a $>60\%$ reduction in viral titers for both H1N1 and H3N2, demonstrating that the identified host factors are important for efficient replication of multiple IAV strains.

To distinguish between IAV-specific host factors and those that function in a pan-proviral manner, we assayed the replication of vesicular stomatitis virus (VSV) in the clonal KOs. VSV replication was unaffected in *SLC35A1* and *PIGN* KOs; however, we observed a >2 log reduction in viral titer in *CIC* KOs and a 50% reduction in viral titer in the remaining KOs (Figure 2C). Taken together, these data suggest that *SLC35A1* and *PIGN* are IAV-specific host factors, whereas *C2CD4C*, *TRIM23*, *CIC*, *JAK2*, and *PIAS3* may function in a pan-proviral manner to support viral replication.

Identification of Viral Life-Cycle Defects in Clonal KO Cells

To elucidate the mechanism by which the identified host factors contribute to IAV replication, we evaluated various stages of the viral life cycle in a subset of clonal KOs. First, to identify host factors that are critical for a single IAV infection cycle, we performed synchronized infections at a high MOI with H5N1. We observed an ~ 1 – 2 log reduction in viral titer in *SLC35A1* and in *CIC* KOs as compared to vector control cells, indicating that loss of these host factors resulted in inefficient establishment or completion of the viral life cycle (Figure 3A). In contrast, the remaining clonal KOs displayed only modest differences in viral titer, suggesting that the defects observed at a low MOI were due to the cumulative effects of multiple replication cycles.

Next, we utilized beta-lactamase carrying influenza virus-like particles (flu VLPs) to measure the ability of the clonal KOs to support virion entry and/or fusion, in comparison to VSV glycoprotein (VSV-G) VLPs (Tscherne et al., 2010). *SLC35A1* KOs showed robust restriction of IAV entry and/or fusion, as only $\sim 3.6\%$ of cells were positive for flu VLP infection (Figure 3B). In addition, only 25% of *PIAS3* KOs were positive for flu VLP

infection, suggesting a role for PIAS3 in IAV entry and/or fusion. In contrast, no defects in flu VLP infection were observed for the remaining KOs, and VSV-G VLP infection was largely unaffected in all of the tested KOs. These results demonstrate that SLC35A1 and PIAS3 play a critical role in the entry and/or fusion stage of the IAV life cycle.

To determine if the remaining host factors are required at a post-fusion stage of the IAV life cycle, we measured primary viral transcription and viral genome replication of H1N1 in the clonal KOs. At 3 hpi, primary nucleoprotein (NP) transcript (NP mRNA) and input viral genomic NP RNA (NP vRNA) levels were measured by qRT-PCR. As *SLC35A1* KOs demonstrated defects in viral entry and/or fusion, we observed low levels of input NP vRNA and consequently low levels of NP transcription as compared to vector control cells (Figure 3C). Interestingly, NP mRNA levels were reduced >90% in *CIC* KOs as compared to vector control cells, despite displaying similar levels of input NP vRNA. Next, we assessed the clonal KOs for defects in viral genome replication at 6 hpi by qRT-PCR. In *CIC* KOs, we observed an ~80% reduction in both NP vRNA and mRNA as compared to vector control cells, indicating that the observed reduction in primary transcription impaired subsequent genome replication. Thus, *CIC* KOs demonstrate a defect in IAV replication at a stage between post-fusion and primary transcription.

As dysregulation of cell-intrinsic immunity may inhibit IAV replication, we evaluated the expression of antiviral genes by qRT-PCR under basal (mock) and H1N1-infected conditions. *CIC* and *JAK2* KOs demonstrated an increase in antiviral gene expression (>2-fold) for both mock and H1N1-infected conditions as compared to vector control cells (Figures 3D, 3E, and S3A). Interestingly, in comparison to vector control cells, *PIAS3* KOs displayed higher antiviral gene expression only upon IAV infection. To further validate our findings, we confirmed the loss of JAK2 protein expression in *JAK2* KOs by western blot analysis (Figure S3B). In addition, we complemented *JAK2* KOs with cDNA expressing *JAK2* and observed increased viral replication (1 log) as compared to GFP expressing *JAK2* KOs, indicating that only loss of the *JAK2* gene resulted in the observed viral replication defects in *JAK2* KOs (Figure S3C). These data demonstrate that *CIC*, *JAK2*, and *PIAS3* KOs display dysregulated antiviral gene expression. Taken together, our studies show that *SLC35A1* KOs display defects in viral entry and/or fusion and *CIC* KOs demonstrate restriction of IAV replication between post-fusion and primary transcription as well as dysregulation of antiviral gene expression.

SLC35A1 Is Required for IAV Entry

IAV infection of a host cell is initiated by the binding of viral HA to sialic acid moieties, which are terminal sugars on glycans (Figure 4A). In our GeCKO screen, we observed enrichment of host factors involved in sialic acid biosynthesis (*GNE*, *CMAS*), transport (*SLC35A1*, *SCL35A2*), glycan modification/processing (*DPM2*, *ALG3*, *ALG4*, *ALG12*, *GANAB*, *A4GALT*, *B3GAT1*, *B4GALNT4*, *CHSY1*, *CSGALNACT2*, and *HS3ST6*) and GPI-anchor synthesis (*PIGN*, *DPM2*) (Figures 4A and S4A). Of these host factors, *SLC35A1* was the highest enriched gene and was represented by 3 independent sgRNAs (Figure S2). As SLC35A1 is a CMP-sialic acid (CMP-Neu5Ac) transporter, we hypothesized that *SLC35A1* KOs lack cell-surface sialic acids (Hadley et al., 2014). To this

end, we used specific lectins to detect 2'-3' (Maackia amurensis lectin [MAL]) or 2'-6' (Sambucus nigra lectin [SNA]) linked sialic acid on the cell surface. Flow cytometry and confocal microscopy analyses of *SLC35A1* KO cells showed a lack of binding for both types of lectins as compared to vector control cells, indicating the loss of cell-surface sialic acid in the absence of *SLC35A1* (Figures 4B and 4C). Next, we evaluated the efficiency of recombinant HA (H5) binding. *SLC35A1* KO cells were unable to support HA binding as compared to vector control cells, indicating that the reduced susceptibility of *SLC35A1* KO cells was due to inefficient binding of IAV particles to the cell surface (Figure 4D).

As there are currently no inhibitors available against SLC35A1, we sought to determine if inhibition of downstream sialyltransferases with 3F-Ax-Peracetyl Neu5Ac (3F-Neu5Ac), a CMP-Neu5Ac analog, would inhibit IAV replication (Rillahan et al., 2012). Treatment of WT A549 cells with 3F-Neu5Ac resulted in robust restriction of H1N1 and H3N2 replication as compared to DMSO-treated cells (Figure 4E). Interestingly, H5N1 replication was unaltered in 3F-Neu5Ac-treated cells, despite displaying almost complete loss of lectin binding (Figure 4F). To exclude the possibility of other defects that may result in the restriction of IAV infection in *SLC35A1* KO cells, we complemented *SLC35A1* KO cells with cDNA expressing *SLC35A1*. We observed increased IAV replication in complemented *SLC35A1* KO cells, yet observed no differences in VSV replication (Figure 4G). In addition, expression of *SLC35A1* in WT A549 cells did not alter IAV replication (Figure S4B). These studies demonstrate that SLC35A1 facilitates incorporation of sialic acid moieties onto cell-surface proteins, and thus is an essential host factor for IAV entry.

Capicua Is a Negative Regulator of Cell-Intrinsic Immunity

Our studies show that capicua (CIC) is critical for both IAV and VSV replication (Figure 2C). CIC is a conserved DNA-binding transcriptional repressor that functions in conjunction with the co-repressor Ataxin1 (ATXN1) or its paralog ATXN1-Like (ATXN1L) (Ajuria et al., 2011; Jiménez et al., 2012). There are two major isoforms of CIC: short (CIC-S) and long (CIC-L), expressed from independent start codons (Figure S5A). To further understand the role of CIC in virus replication, we first confirmed our findings in new *CIC* KO cells generated with an independent sgRNA (*CIC* KO2s). Loss of CIC expression in *CIC* KO2s was confirmed by western blot analysis and sequencing of the sgRNA target site (Figure S5B; Table S5). In agreement with previous findings, we observed decreased levels of ATXN1L protein as well as increased expression of a CIC-regulated gene, *ETV4*, in *CIC* KO2s (Figure S5B and S5C) (Dissanayake et al., 2011; Lee et al., 2011). As previously observed, *CIC* KO2s also demonstrated an ~2-3 log reduction in the replication of various IAV strains, as well as a 1 log reduction in VSV, encephalomyocarditis virus (EMCV), and Zika virus replication (Figures 2C and 5A). As anticipated, we observed higher antiviral gene expression in *CIC* KO2s under basal (mock) and H1N1-infected conditions as compared to vector control cells (Figures 5B-5D). Together, these data suggest that loss of *CIC* results in a heightened antiviral state, rendering cells less permissive to viral replication.

As loss of *CIC* resulted in higher antiviral gene expression, we hypothesized that ectopic expression of *CIC* would suppress the activity of antiviral gene promoters. Thus, we generated luciferase reporters under the control of the human *IFIT1* and *MxA* promoters.

Co-expression of *CIC* and *ATXN1* resulted in a dose dependent decrease in IFIT1 reporter activity (up to ~50%) upon RIG-I stimulation as compared to GFP control, to a greater extent than expression of *CIC* or *ATXN1* alone (Figure 5E). Similarly, an ~40% reduction in MxA reporter activity was observed upon co-expression of *CIC* and *ATXN1*. As our results indicate that *CIC* can repress antiviral gene expression, we investigated if downregulation of *CIC* occurs upon infection to facilitate the induction of antiviral genes.

Western blot analysis of H1N1-infected vector control cells demonstrated a rapid decline in *CIC* protein levels between 40–60 min post-infection (Figure 5F). qRT-PCR analysis of H1N1-infected vector control cells showed an ~50% decrease in *CIC* mRNA levels, demonstrating that both *CIC* mRNA and protein levels are downregulated in response to IAV infection (Figure 5G). Taken together, GeCKO screening has identified *CIC* as a negative regulator of cell-intrinsic immunity.

DISCUSSION

Here, we performed a GeCKO screen using a human isolate of an avian H5N1 strain and identified host factors critical for IAV entry and regulation of cell-intrinsic immunity. Cells lacking the sialic acid transporter *SLC35A1* were highly enriched post-H5N1 selection, as they were deficient in the viral receptor and thus were incapable of supporting HA binding. sgRNAs targeting several genes involved in sialic acid biosynthesis and related glycosylation pathways were also enriched during H5N1 selection. In addition, we identified *CIC*, a DNA-binding transcriptional repressor, as a key regulator of cell-intrinsic immunity. *CIC*-deficient cells demonstrated upregulated antiviral gene expression and decreased replication of multiple viruses. Taken together, GeCKO screening can be a powerful tool to discover host factors and to highlight biological pathways essential for the replication of intracellular pathogens.

For this study, we employed a pooled GeCKO approach, relying upon gene disruption and stringent selection to enrich for a cell population resistant to IAV infection. As opposed to siRNA-based screening, it has been reported that cell-survival-based GeCKO screens for viral host factors predominantly reveal hits that support early steps of viral replication (Perreira et al., 2016; Savidis et al., 2016). Similarly, we observed robust enrichment of host factors important for sialic acid (IAV receptor) expression as well as vacuolar acidification and endocytosis (Figure 1E; Table S3). Of these identified entry factors, several members of the vacuolar ATPase family were previously identified in multiple siRNA screens (Mehle and Doudna, 2010; Stertz and Shaw, 2011b; Watanabe et al., 2010; Figure 1D; Table S2). Interestingly, *SLC35A1* was identified in only one of the prior siRNA screens, and knockdown demonstrated an ~50% decrease in H1N1 (PR8) infection (Brass et al., 2009). In this GeCKO screen, *SLC35A1* was the highest enriched hit and gene knockout displayed an ~5 log decrease in viral replication for multiple IAV strains (Figure 2C). In addition, several host factors critical for sialic acid biosynthesis and related glycosylation pathways were uniquely enriched in this GeCKO screen (Figures 4A and S4A) (Chu and Whittaker, 2004; de Vries et al., 2012). In agreement, a survival-based haploid screen for enterovirus D68, which also utilizes sialic acid as an entry receptor, showed enrichment of host factors necessary for cell-surface sialic acid expression (Baggen et al., 2016). Thus, survival-based

GeCKO screening allows for the identification of host factors critical for the early steps of viral replication.

In addition to the identification of viral entry host factors, GeCKO screening revealed factors important for the regulation of cell-intrinsic immunity. In our validation studies, we observed higher levels of antiviral gene expression in *CIC*, *JAK2*, and *PIAS3* KOs (Figures 3D and 3E); however, loss of these host factors impacted different steps of the IAV life cycle (Figures 3A–3C). *JAK2* was previously identified in one of the siRNA screens and implicated in IAV entry (König et al., 2010). However, in *JAK2* KOs, we observed no defects in flu VLP entry yet decreased genome replication at 6 hpi. It is possible that increased antiviral gene expression may suppress IAV genome replication in *JAK2* KOs. In another study, *JAK2* was implicated in the intracellular localization of the viral M1 protein through tyrosine phosphorylation (König et al., 2010; Wang et al., 2013). Therefore, further studies are necessary to delineate the role of *JAK2* in IAV replication. In *PIAS3* KOs, we observed increased antiviral gene expression only upon IAV infection, as well as defects in flu VLP entry and primary transcription. Interestingly, *PIAS3*, an E3 SUMO ligase, has been shown to SUMOylate *RAC1* and modulate cytoskeletal rearrangement; thus, it is possible that *PIAS3* plays a role in IAV endocytosis (Castillo-Lluva et al., 2010). In addition, it has previously been shown that *PIAS1* and *PIAS3* negatively regulate *STAT*-mediated signaling and *IRF1* transcriptional activity, suggesting that *PIAS3* may be important for modulating cell-intrinsic immunity (Nakagawa and Yokosawa, 2002). These findings suggest that *JAK2* and *PIAS3* are important for the regulation of cell-intrinsic immunity, yet may function at different steps of the IAV life cycle.

CIC in conjunction with the co-repressor Ataxin1 (*ATXN1*) or its paralog *ATXN1*-like (*ATXN1L*) has been implicated in cancer development and progression, as well as neuropathology and autoimmunity (Bettegowda et al., 2011; Lam et al., 2006; Okimoto et al., 2017; Park et al., 2017b). However, *CIC* has not been shown to play a role in the regulation of cell-intrinsic immunity. In our validation studies, we observed robust restriction of RNA viruses from diverse families and increased antiviral gene expression in *CIC* KO2s (Figures 5A–5D). In agreement, a previous study demonstrated increased levels of proinflammatory cytokines in *CIC*-L-deficient mice (Kim et al., 2015). In addition, we observed repression of *IFIT1* and *MxA* reporter activity upon ectopic expression of *CIC* with the co-repressor *ATXN1* (Figure 5E). As *CIC* has been previously demonstrated to function as a DNA-binding transcriptional repressor, it is possible that *CIC* suppresses antiviral gene expression via its transcriptional repressor activity (Jiménez et al., 2012). Furthermore, our studies demonstrate downregulation of *CIC* protein and RNA levels upon IAV infection (Figures 5F and 5G). As viral infections activate *MAPK* pathways, and the activation of *MAPK* pathways result in the downregulation of *CIC*, it is possible that *CIC* degradation during IAV infection occurs via *MAPK* signaling (Ajuria et al., 2011; Dissanayake et al., 2011; Pleschka, 2008). Previous studies show that *CIC* degradation can be inhibited by the *COP9* signalosome (Suisse et al., 2017). Interestingly, multiple members of the *COP9* complex have been identified as IAV host factors; thus, it is tempting to speculate that viruses may usurp the *COP9* signalosome to prevent *CIC* degradation and thereby repress host antiviral gene expression (Tripathi et al., 2015). Future studies will determine the mechanisms of *CIC* regulation during viral infection.

In conclusion, GeCKO screening is a powerful alternative strategy for the identification of host factors and biological pathways critical for the replication of multiple influenza viruses. Host pathways required for expression of the viral receptor sialic acid were uniquely enriched in this GeCKO screen, with the highest enrichment observed for SLC35A1, a sialic acid transporter. In addition to highlighting biological pathways, our GeCKO screen identified CIC as a host factor important for the regulation of cell-intrinsic immunity. Our studies show that CIC suppresses antiviral gene expression and suggest that CIC levels are regulated during viral infection to facilitate robust induction of antiviral responses. Therefore, we demonstrate that GeCKO screening is an invaluable tool for the discovery of host factors essential for the replication of intracellular pathogens and for the identification of targets for the development of host-directed therapeutics.

EXPERIMENTAL PROCEDURES

A549-GeCKO Library Generation and H5N1 Screen

The A549-GeCKO library was generated using the lentiGuide-Puro (#52963, Addgene) two-vector system for Cas9 and sgRNA delivery as previously described (Sanjana et al., 2014). Briefly, Cas9-A549 cells were generated via lentivirus transduction of the Cas9 transgene (lentiCas9-BLAST, #52962, Addgene), followed by selection with 5 µg/ml blasticidin. Clonal Cas9-A549 cells were further transduced with lentivirus particles containing the human sgRNA library (Human GeCKO v2 Library A Cat#1000000049, Addgene) at MOI = 0.3 to attain no greater than 1 sgRNA per cell and selected with both 1 µg/ml puromycin and 5 µg/ml blasticidin for 14 days to achieve >95% gene disruption (Shalem et al., 2014). For the preliminary consecutive screen, 2×10^8 A549-GeCKO library cells were infected with VN04_{Low} (H5N1) at MOI = 5 in infection media for 2 days. Surviving cells were reseeded in DMEM supplemented with 10% fetal bovine serum (FBS) and 1% penicillin/streptomycin (P/S) solution and subjected to four more rounds of infection. The surviving resistant population was expanded to 1×10^7 cells and subjected to deep sequencing analysis. For the sequential screen, 2×10^8 A549-GeCKO library cells were infected with VN04_{Low} (H5N1) at MOI = 5 in infection media for 2 days in biological duplicates, and the surviving cells were allowed to expand ($\sim 2-4 \times 10^7$). One-fifth of the expanded cells were utilized for deep sequencing analysis, and four-fifths of the expanded cells were subjected to the next round of infection.

Statistical Analysis

Statistical significance was determined by two-tailed unpaired Student's t test, and p values 0.05 are considered significant and denoted with an asterisk. Non-significant values are denoted as ns.

Additional experimental procedures are included in the Supplemental Experimental Procedures.

Supplementary Material

Refer to Web version on PubMed Central for supplementary material.

Acknowledgments

We are grateful to Dr. Adolfo Garcia-Sastre (Icahn School of Medicine) for numerous reagents, and a special thank you to Dr. Feng Zhang (MIT) for kindly sharing the human GeCKO library (Addgene). Imaging was performed at The University of Chicago Integrated Light Microscopy Core Facility. We would like to thank Dr. Pieter Faber at The University of Chicago Genomic Facility for help with deep sequencing. J.H. is supported by the NIH Molecular and Cellular Biology training program at The University of Chicago (T32GM007183) and NIH Diversity Supplement (R01AI123359-02S1). B.M. is supported by NIAID grants (R01AI123359 and R01AI127775). J.A. is supported by the NIH National Center for Advancing Translational Sciences (UL1 TR000430).

References

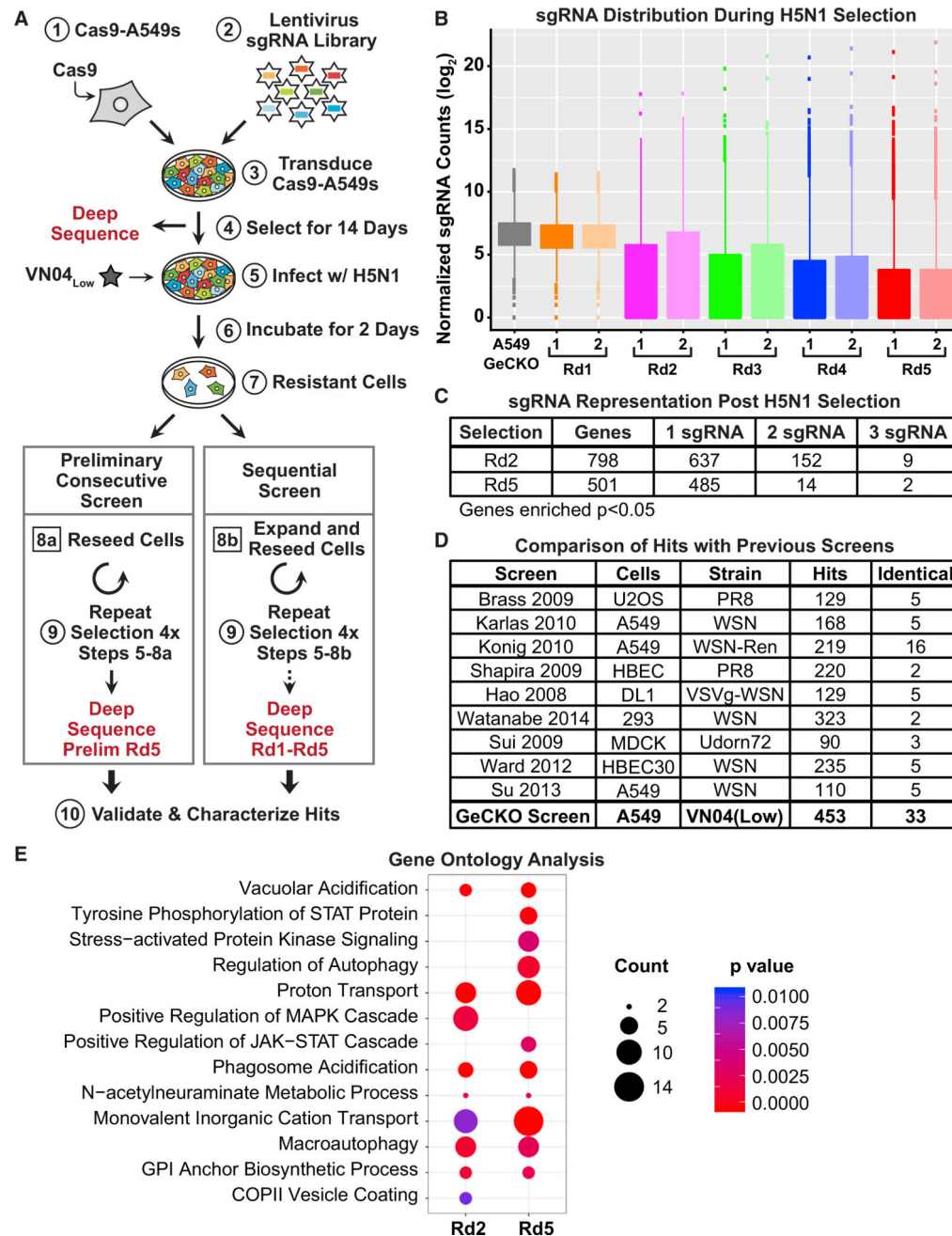
- Ajuria L, Nieva C, Winkler C, Kuo D, Samper N, Andreu MJ, Helman A, González-Crespo S, Paroush Z, Courey AJ, Jiménez G. Capicua DNA-binding sites are general response elements for RTK signaling in *Drosophila*. *Development*. 2011; 138:915–924. [PubMed: 21270056]
- Baggen J, Thibaut HJ, Staring J, Jae LT, Liu Y, Guo H, Slager JJ, de Bruin JW, van Vliet AL, Blomen VA, et al. Enterovirus D68 receptor requirements unveiled by haploid genetics. *Proc. Natl. Acad. Sci. USA*. 2016; 113:1399–1404. [PubMed: 26787879]
- Benitez AA, Panis M, Xue J, Varble A, Shim JV, Frick AL, López CB, Sachs D, tenOever BR. In vivo RNAi screening identifies MDA5 as a significant contributor to the cellular defense against influenza A virus. *Cell Rep*. 2015; 11:1714–1726. [PubMed: 26074083]
- Bettegowda C, Agrawal N, Jiao Y, Sausen M, Wood LD, Hruban RH, Rodriguez FJ, Cahill DP, McLendon R, Riggins G, et al. Mutations in CIC and FUBP1 contribute to human oligodendroglioma. *Science*. 2011; 333:1453–1455. [PubMed: 21817013]
- Brass AL, Huang IC, Benita Y, John SP, Krishnan MN, Feeley EM, Ryan BJ, Weyer JL, van der Weyden L, Fikrig E, et al. The IFITM proteins mediate cellular resistance to influenza A H1N1 virus, West Nile virus, and dengue virus. *Cell*. 2009; 139:1243–1254. [PubMed: 20064371]
- Castillo-Lluva S, Tatham MH, Jones RC, Jaffray EG, Edmondson RD, Hay RT, Malliri A. SUMOylation of the GTPase Rac1 is required for optimal cell migration. *Nat. Cell Biol*. 2010; 12:1078–1085. [PubMed: 20935639]
- Chu VC, Whittaker GR. Influenza virus entry and infection require host cell N-linked glycoprotein. *Proc. Natl. Acad. Sci. USA*. 2004; 101:18153–18158. [PubMed: 15601777]
- de Vries E, de Vries RP, Wienholts MJ, Floris CE, Jacobs MS, van den Heuvel A, Rottier PJ, de Haan CA. Influenza A virus entry into cells lacking sialylated N-glycans. *Proc. Natl. Acad. Sci. USA*. 2012; 109:7457–7462. [PubMed: 22529385]
- Dissanayake K, Toth R, Blakey J, Olsson O, Campbell DG, Prescott AR, MacKintosh C. ERK/p90(RSK)/14-3-3 signalling has an impact on expression of PEA3 Ets transcription factors via the transcriptional repressor capicúa. *Biochem. J*. 2011; 433:515–525. [PubMed: 21087211]
- Hadley B, Maggioni A, Ashikov A, Day CJ, Haselhorst T, Tiralongo J. Structure and function of nucleotide sugar transporters: current progress. *Comput. Struct. Biotechnol. J*. 2014; 10:23–32. [PubMed: 25210595]
- Haga K, Fujimoto A, Takai-Todaka R, Miki M, Doan YH, Murakami K, Yokoyama M, Murata K, Nakanishi A, Katayama K. Functional receptor molecules CD300lf and CD300ld within the CD300 family enable murine noroviruses to infect cells. *Proc. Natl. Acad. Sci. USA*. 2016; 113:E6248–E6255. [PubMed: 27681626]
- Hao L, Sakurai A, Watanabe T, Sorensen E, Nidom CA, Newton MA, Ahlquist P, Kawaoka Y. *Drosophila* RNAi screen identifies host genes important for influenza virus replication. *Nature*. 2008; 454:890–893. [PubMed: 18615016]
- Jiménez G, Shvartsman SY, Paroush Z. The Capicua repressor—a general sensor of RTK signaling in development and disease. *J. Cell Sci*. 2012; 125:1383–1391. [PubMed: 22526417]
- Karlas A, Machuy N, Shin Y, Pleissner KP, Artarini A, Heuer D, Becker D, Khalil H, Ogilvie LA, Hess S, et al. Genome-wide RNAi screen identifies human host factors crucial for influenza virus replication. *Nature*. 2010; 463:818–822. [PubMed: 20081832]
- Kim E, Park S, Choi N, Lee J, Yoe J, Kim S, Jung HY, Kim KT, Kang H, Fryer JD, et al. Deficiency of Capicua disrupts bile acid homeostasis. *Sci. Rep*. 2015; 5:8272. [PubMed: 25653040]

- König R, Stertz S, Zhou Y, Inoue A, Hoffmann HH, Bhattacharyya S, Alamares JG, Tscherne DM, Ortigoza MB, Liang Y, et al. Human host factors required for influenza virus replication. *Nature*. 2010; 463:813–817. [PubMed: 20027183]
- Lam YC, Bowman AB, Jafar-Nejad P, Lim J, Richman R, Fryer JD, Hyun ED, Duvick LA, Orr HT, Botas J, Zoghbi HY. ATAXIN-1 interacts with the repressor Capicua in its native complex to cause SCA1 neuropathology. *Cell*. 2006; 127:1335–1347. [PubMed: 17190598]
- Lee Y, Fryer JD, Kang H, Crespo-Barreto J, Bowman AB, Gao Y, Kahle JJ, Hong JS, Kheradmand F, Orr HT, et al. ATXN1 protein family and CIC regulate extracellular matrix remodeling and lung alveolarization. *Dev. Cell*. 2011; 21:746–757. [PubMed: 22014525]
- Li W, Xu H, Xiao T, Cong L, Love MI, Zhang F, Irizarry RA, Liu JS, Brown M, Liu XS. MAGeCK enables robust identification of essential genes from genome-scale CRISPR/Cas9 knockout screens. *Genome Biol*. 2014; 15:554. [PubMed: 25476604]
- Ma H, Dang Y, Wu Y, Jia G, Anaya E, Zhang J, Abraham S, Choi JG, Shi G, Qi L, et al. A CRISPR-based screen identifies genes essential for West-Nile-virus-induced cell death. *Cell Rep*. 2015; 12:673–683. [PubMed: 26190106]
- Marceau CD, Puschnik AS, Majzoub K, Ooi YS, Brewer SM, Fuchs G, Swaminathan K, Mata MA, Elias JE, Sarnow P, Carette JE. Genetic dissection of Flaviviridae host factors through genome-scale CRISPR screens. *Nature*. 2016; 535:159–163. [PubMed: 27383987]
- Mehle A, Doudna JA. A host of factors regulating influenza virus replication. *Viruses*. 2010; 2:566–573. [PubMed: 21994648]
- Nakagawa K, Yokosawa H. PIAS3 induces SUMO-1 modification and transcriptional repression of IRF-1. *FEBS Lett*. 2002; 530:204–208. [PubMed: 12387893]
- Okimoto RA, Breitenbuecher F, Olivas VR, Wu W, Gini B, Hofree M, Asthana S, Hrustanovic G, Flanagan J, Tulpule A, et al. Inactivation of Capicua drives cancer metastasis. *Nat. Genet*. 2017; 49:87–96. [PubMed: 27869830]
- Orchard RC, Wilen CB, Doench JG, Baldrige MT, McCune BT, Lee YC, Lee S, Pruett-Miller SM, Nelson CA, Fremont DH, Virgin HW. Discovery of a proteinaceous cellular receptor for a norovirus. *Science*. 2016; 353:933–936. [PubMed: 27540007]
- Park RJ, Wang T, Koundakjian D, Hultquist JF, Lamothe-Molina P, Monel B, Schumann K, Yu H, Krupczak KM, Garcia-Beltran W, et al. A genome-wide CRISPR screen identifies a restricted set of HIV host dependency factors. *Nat. Genet*. 2017a; 49:193–203. [PubMed: 27992415]
- Park S, Lee S, Lee CG, Park GY, Hong H, Lee JS, Kim YM, Lee SB, Hwang D, Choi YS, et al. Capicua deficiency induces autoimmunity and promotes follicular helper T cell differentiation via derepression of ETV5. *Nat. Commun*. 2017b; 8:16037. [PubMed: 28855737]
- Perreira JM, Meraner P, Brass AL. functional genomic strategies for elucidating human-virus interactions: will CRISPR knockout RNAi and haploid cells? *Adv. Virus Res*. 2016; 94:1–51. [PubMed: 26997589]
- Pleschka S. RNA viruses and the mitogenic Raf/MEK/ERK signal transduction cascade. *Biol. Chem*. 2008; 389:1273–1282. [PubMed: 18713014]
- Rillahan CD, Antonopoulos A, Lefort CT, Sonon R, Azadi P, Ley K, Dell A, Haslam SM, Paulson JC. Global metabolic inhibitors of sialyl- and fucosyltransferases remodel the glycome. *Nat. Chem. Biol*. 2012; 8:661–668. [PubMed: 22683610]
- Sanjana NE, Shalem O, Zhang F. Improved vectors and genome-wide libraries for CRISPR screening. *Nat. Methods*. 2014; 11:783–784. [PubMed: 25075903]
- Savidis G, McDougall WM, Meraner P, Perreira JM, Portmann JM, Trincucci G, John SP, Aker AM, Renzette N, Robbins DR, et al. Identification of Zika virus and dengue Virus dependency factors using functional genomics. *Cell Rep*. 2016; 16:232–246. [PubMed: 27342126]
- Shalem O, Sanjana NE, Hartenian E, Shi X, Scott DA, Mikkelsen T, Heckl D, Ebert BL, Root DE, Doench JG, Zhang F. Genome-scale CRISPR-Cas9 knockout screening in human cells. *Science*. 2014; 343:84–87. [PubMed: 24336571]
- Shapira SD, Gat-Viks I, Shum BO, Dricot A, de Grace MM, Wu L, Gupta PB, Hao T, Silver SJ, Root DE, et al. A physical and regulatory map of host-influenza interactions reveals pathways in H1N1 infection. *Cell*. 2009; 139:1255–1267. [PubMed: 20064372]

- Stertz S, Shaw ML. Uncovering the global host cell requirements for influenza virus replication via RNAi screening. *Microbes Infect.* 2011; 13:516–525. [PubMed: 21276872]
- Su WC, Chen YC, Tseng CH, Hsu PW, Tung KF, Jeng KS, Lai MM. Pooled RNAi screen identifies ubiquitin ligase Itch as crucial for influenza A virus release from the endosome during virus entry. *Proc. Natl. Acad. Sci. USA.* 2013; 110:17516–17521. [PubMed: 24101521]
- Sui B, Bamba D, Weng K, Ung H, Chang S, Van Dyke J, Goldblatt M, Duan R, Kinch MS, Li WB. The use of random homozygous gene perturbation to identify novel host-oriented targets for influenza. *Virology.* 2009; 387:473–481. [PubMed: 19327807]
- Suisse A, He D, Legent K, Treisman JE. COP9 signalosome subunits protect Capicua from MAPK-dependent and -independent mechanisms of degradation. *Development.* 2017; 144:2673–2682. [PubMed: 28619822]
- Tripathi S, Pohl MO, Zhou Y, Rodriguez-Frandsen A, Wang G, Stein DA, Moulton HM, DeJesus P, Che J, Mulder LC, et al. Meta-and orthogonal integration of influenza “OMICs” data defines a role for UBR4 in virus budding. *Cell Host Microbe.* 2015; 18:723–735. [PubMed: 26651948]
- Tscherne DM, Manicassamy B, García-Sastre A. An enzymatic virus-like particle assay for sensitive detection of virus entry. *J. Virol. Methods.* 2010; 163:336–343. [PubMed: 19879300]
- Wang S, Zhao Z, Bi Y, Sun L, Liu X, Liu W. Tyrosine 132 phosphorylation of influenza A virus M1 protein is crucial for virus replication by controlling the nuclear import of M1. *J. Virol.* 2013; 87:6182–6191. [PubMed: 23536660]
- Wang T, Wei JJ, Sabatini DM, Lander ES. Genetic screens in human cells using the CRISPR-Cas9 system. *Science.* 2014; 343:80–84. [PubMed: 24336569]
- Ward SE, Kim HS, Komurov K, Mendiratta S, Tsai PL, Schmolke M, Satterly N, Manicassamy B, Forst CV, Roth MG, et al. Host modulators of H1N1 cytopathogenicity. *PLoS ONE.* 2012; 7:e39284. [PubMed: 22876275]
- Watanabe T, Watanabe S, Kawaoka Y. Cellular networks involved in the influenza virus life cycle. *Cell Host Microbe.* 2010; 7:427–439. [PubMed: 20542247]
- Watanabe T, Kawakami E, Shoemaker JE, Lopes TJ, Matsuoka Y, Tomita Y, Kozuka-Hata H, Gorai T, Kuwahara T, Takeda E, et al. Influenza virus-host interactome screen as a platform for antiviral drug development. *Cell Host Microbe.* 2014; 16:795–805. [PubMed: 25464832]
- Wright PF, Neumann G, Kawaoka Y. Orthomyxoviruses. In: Knipe DM, Howley PM, editors. *Fields Virology.* Lippincott Williams & Wilkins; 2013.
- Wright AV, Nuñez JK, Doudna JA. Biology and applications of CRISPR systems: harnessing nature’s toolbox for genome engineering. *Cell.* 2016; 164:29–44. [PubMed: 26771484]
- Yu G, He QY. ReactomePA: an R/Bioconductor package for reactome pathway analysis and visualization. *Mol. Biosyst.* 2016; 12:477–479. [PubMed: 26661513]
- Zhang R, Miner JJ, Gorman MJ, Rausch K, Ramage H, White JP, Zuiani A, Zhang P, Fernandez E, Zhang Q, et al. A CRISPR screen defines a signal peptide processing pathway required by flaviviruses. *Nature.* 2016; 535:164–168. [PubMed: 27383988]

Highlights

- Genome-wide CRISPR/Cas9 screen used to identify pro-viral IAV host factors
- Host factors identified in viral entry and regulation of antiviral gene expression
- Sialic acid transporter SLC35A1 is essential for viral receptor expression
- Transcriptional repressor CIC is a negative regulator of cell-intrinsic immunity



of H5N1 infection with substantial expansion of resistant cells between each round. Step 10: validation and characterization of selected hits.

(B) Boxplot of sgRNA distribution in the A549-GeCKO library and after each round (Rd) of the sequential screen. Biological replicates are shown as Rep1 and Rep2; values are represented in \log_2 scale; and sgRNAs are median-normalized to account for differences in total Illumina read counts. Each point represents individual sgRNAs. sgRNAs are distributed by quartile, where the boxes represent the middle quartiles (25%–75% distribution), and the lines and dots represent sgRNAs in the upper and the lower 25% of the distribution.

(C) Summary of genes enriched at Rd2 and Rd5 of the sequential screen. sgRNAs enriched during H5N1 selection were identified using the MAGeCK program ($p < 0.05$) and mapped to corresponding genes.

(D) Comparison of hits identified at Rd5 of the sequential screen, excluding miRNAs, with nine genome-wide screens performed for IAV. See also Table S2.

(E) Gene ontology analysis of Rd2 and Rd5 hits from the sequential screen, excluding miRNAs.

See also Figure S1.

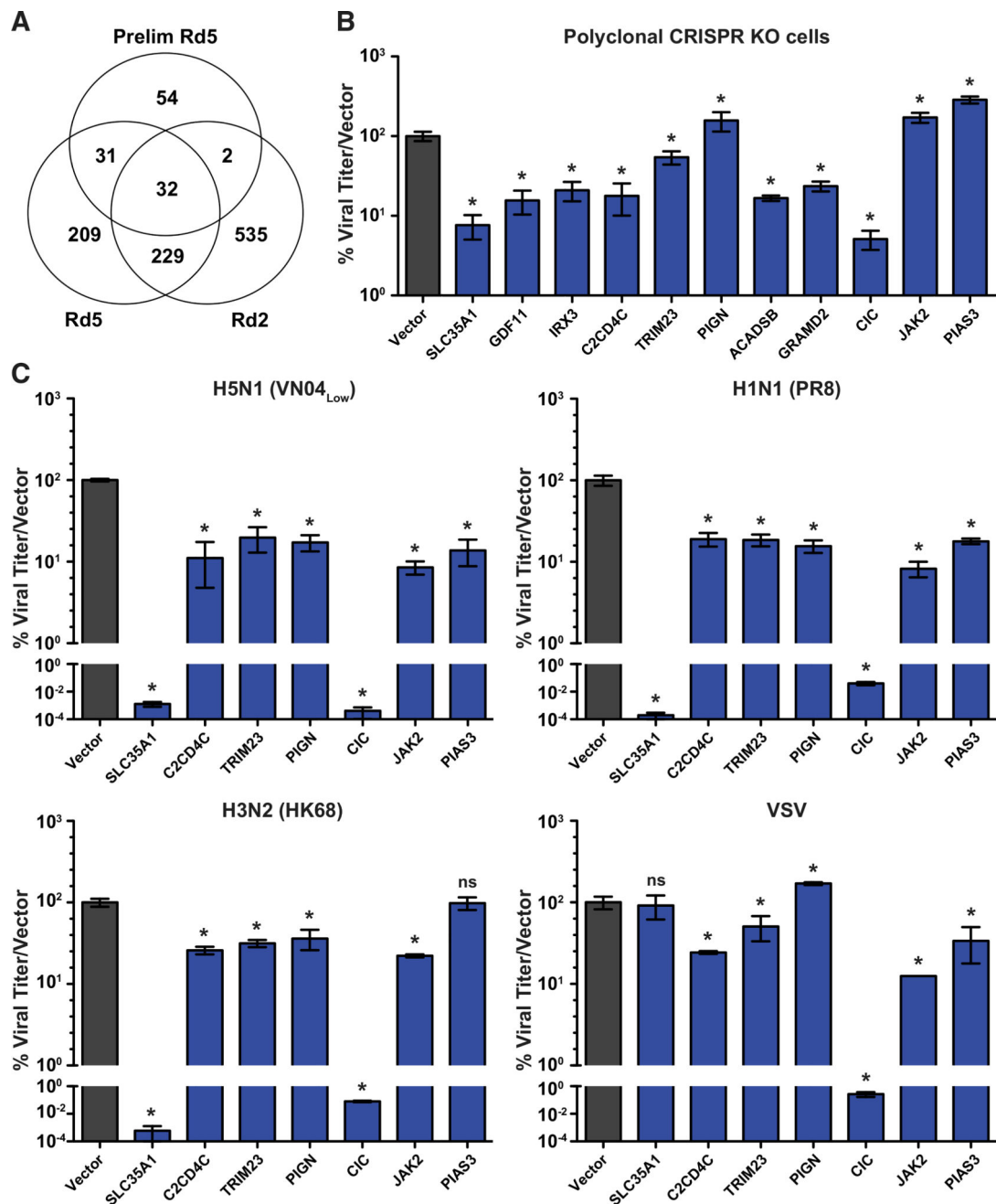


Figure 2. Validation of Selected Hits with Multiple IAV Strains

(A) Venn diagram representation of overlapping hits identified in the preliminary consecutive screen (Prelim Rd5) and Rd2 and Rd5 of the sequential screen. See also Table S4.

(B) Validation of individual hits. Vector control and polyclonal KOs were infected with H5N1 (MOI = 0.001), and viral titers were measured at 48 hpi.

(C) Comparison of viral replication. Vector control and clonal KOs were infected with H5N1 (MOI = 0.001), H1N1 (MOI = 0.01), H3N2 (MOI = 0.01), and VSV (MOI = 0.001), and viral titers were measured at 48 hpi. Data are represented as a percentage mean titer of

triplicate samples relative to vector control cells \pm SD. * $p < 0.05$; ns, non-significant. Data are representative of at least three independent experiments. See also Figure S2.

Author Manuscript

Author Manuscript

Author Manuscript

Author Manuscript

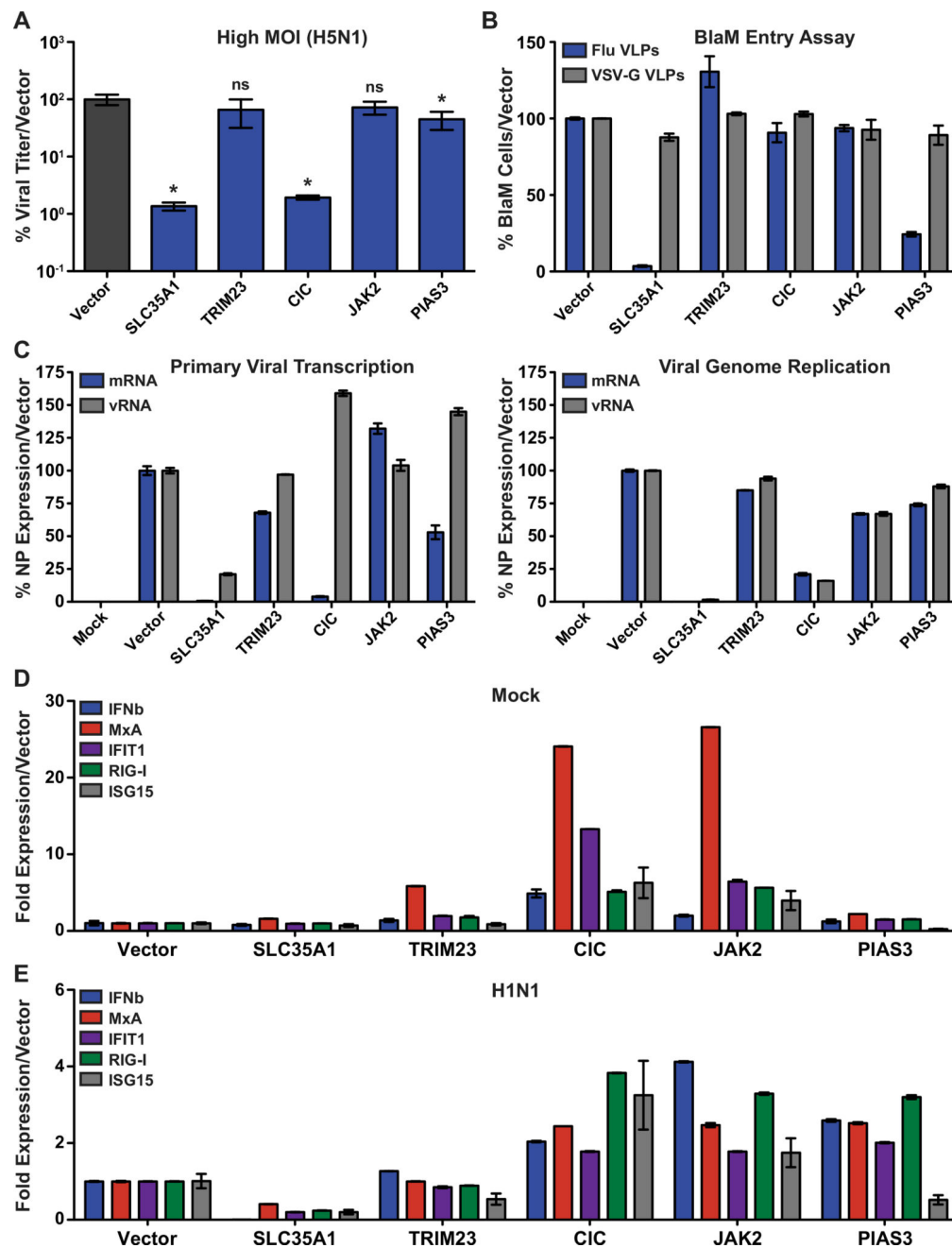


Figure 3. Identification of Viral Life-Cycle Defects for Selected Hits

(A) Comparison of viral replication at a high MOI. Vector control and clonal KO cells were infected with H5N1 (MOI = 1), and viral titers were measured at 24 hpi. Data are represented as a percentage mean titer of triplicate samples relative to vector control cells \pm SD. * $p < 0.05$; ns, non-significant.

(B) BlaM VLP entry assay. Vector control and clonal KO cells were infected with flu VLPs (HA/NA) or VSV-G VLPs containing a β -lactamase-M1 fusion protein and analyzed by flow cytometry. Values are represented as a percentage of vector control cells \pm SD.

(C) qRT-PCR analysis of primary viral transcription and viral genome replication. Vector control and clonal KOs were infected with H1N1 (MOI = 3) and NP mRNA, and vRNA levels were analyzed at 3 hpi (cycloheximide pretreatment; primary viral transcription) or at 6 hpi (untreated; viral genome replication). Data are represented as a percentage of expression relative to H1N1-infected vector control cells \pm SD.

(D and E) qRT-PCR analysis of antiviral gene expression in basal (mock) or in H1N1-infected conditions. Vector control and clonal KOs were infected with H1N1 (MOI = 5), and mRNA levels for the indicated genes were measured at 16 hpi. Data are represented as the fold expression relative to uninfected (mock) vector control cells \pm SD (D) or H1N1-infected vector control cells \pm SD (E).

Data are representative of at least three independent experiments.

See also Figure S3.

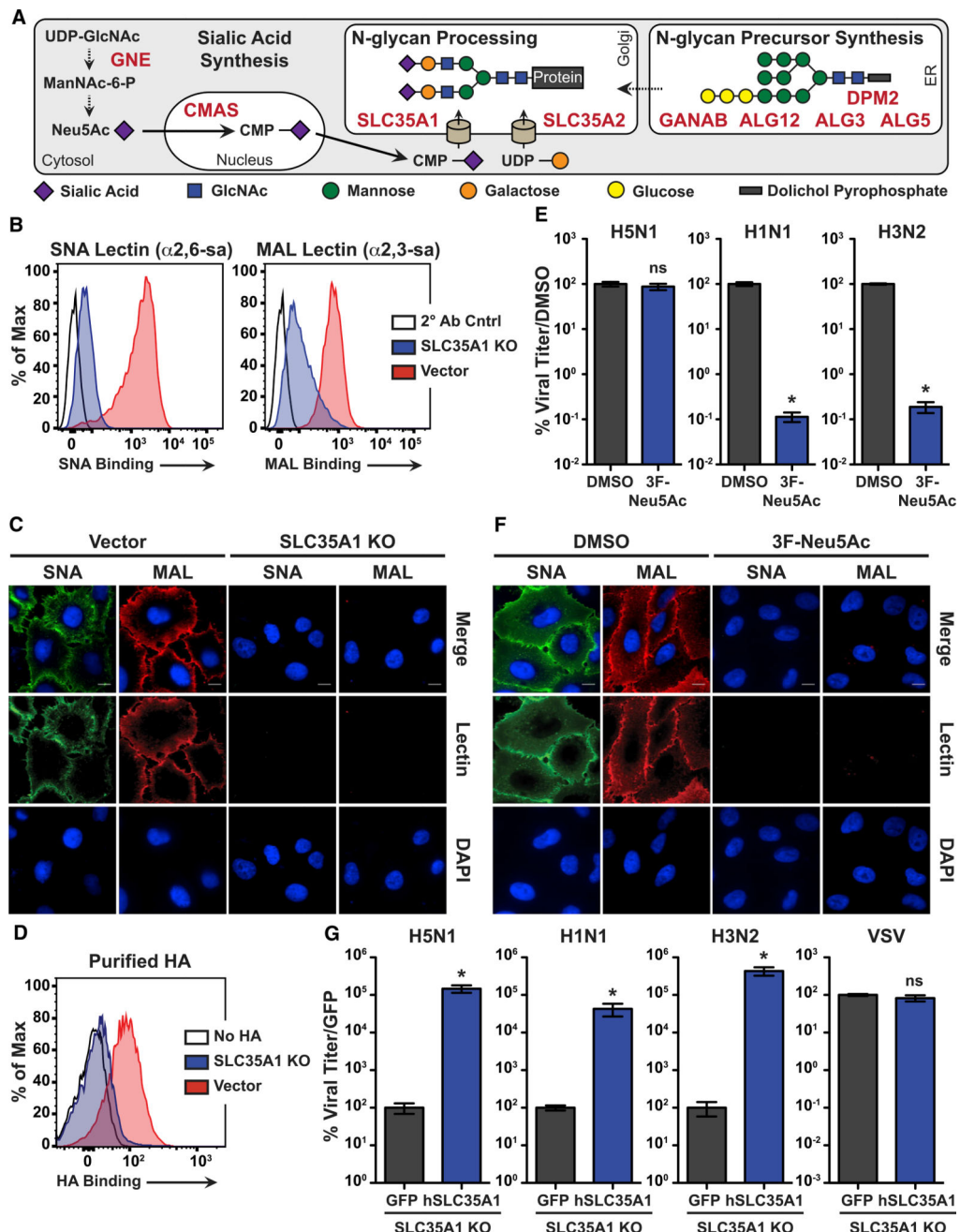


Figure 4. Sialic Acid Transporter SLC35A1 Is Required for IAV Entry

(A) Simplified schematic of *de novo* sialic acid biosynthesis and N-glycan processing pathway. Significant genes identified in the GeCKO screen are shown in red. N-acetylglucosamine (GlcNAc), N-acetylmannosamine (ManNAc), and N-acetylneuraminic acid (Neu5Ac), cytidine monophosphate (CMP), and uridine diphosphate (UDP). (B and C) Analysis of sialic acid expression by lectin staining. Vector control and *SLC35A1* KOs were treated with lectins that have specificity for 2'-6' (SNA) or 2'-3' (MAL) sialic acids and analyzed by flow cytometry (B) and fluorescent microscopy (C). Histograms depict the intensity of lectin binding relative to cell count. Scale bar, 10 μ m.

(D) Quantification of HA binding. Vector control and *SLC35A1* KOs were incubated with purified HA (H5) and analyzed by flow cytometry.

(E) Treatment with sialic acid analog decreases IAV replication. WT A549s were treated with DMSO or 200 μ M 3Fax-Peracetyl Neu5Ac (3F-Neu5Ac) for 10 days and infected with the indicated viruses (MOI = 0.1), and viral titers were measured at 18 hpi.

(F) Fluorescent microscopy of lectin binding in 3F-Neu5Ac-treated WT A549 cells. SNA and MAL staining was performed as described for (C). Scale bar, 10 μ m.

(G) Complementation with *SLC35A1* cDNA restores IAV replication. *SLC35A1* KOs complemented with GFP- or hSLC35A1-expressing vector were infected with H5N1 (MOI = 0.001), H1N1 (MOI = 0.01), H3N2 (MOI = 0.01), and VSV (MOI = 0.001), and viral titers were measured at 48 hpi.

Data are represented as mean percentage titer of triplicate samples relative to DMSO-treated WT A549 cells \pm SD (E) or GFP-expressing *SLC35A1* KOs \pm SD (G). * $p < 0.05$; ns, non-significant. Data are representative of at least three independent experiments.

See also Figure S4.

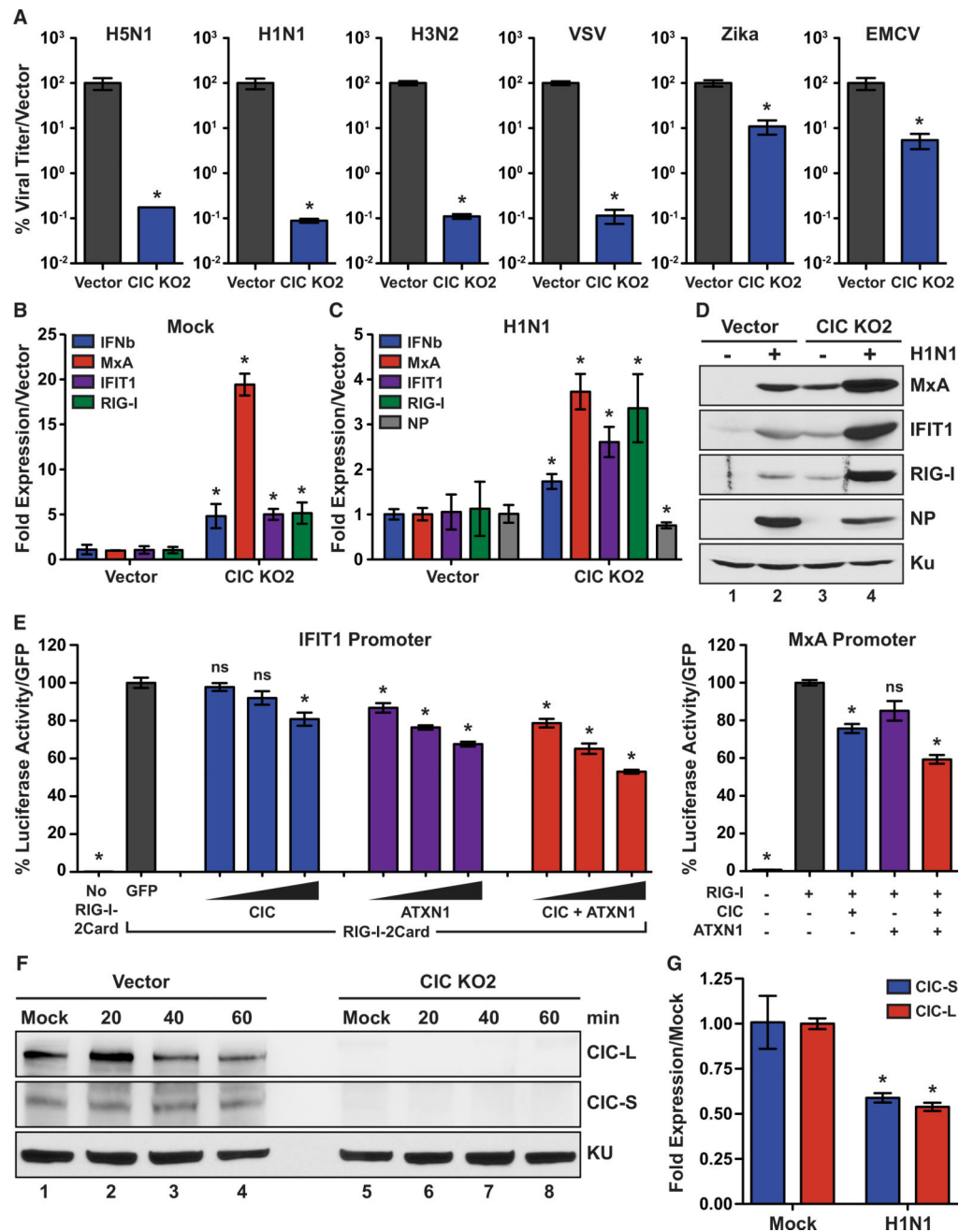


Figure 5. CIC Is a Negative Regulator of Antiviral Gene Expression

(A) Comparison of viral replication. Vector control or *CIC* KO2s were infected with H5N1 (MOI = 0.001), H1N1 (MOI = 0.01), H3N2 (MOI = 0.01), VSV (MOI = 0.001), Zika virus (MOI = 0.01), and EMCV (MOI = 0.05) and viral titers were measured at 48 hpi (EMCV at 24 hpi). Data are represented as a percentage mean titer of triplicate samples relative to vector control cells \pm SD.

(B and C) qRT-PCR analysis of antiviral gene expression in basal (mock) or in H1N1-infected conditions. Vector control and *CIC* KO2s were infected with H1N1 (MOI = 5), and mRNA levels for the indicated genes were measured at 16 hpi. Data are represented as the

fold expression relative to uninfected (mock) vector control cells \pm SD (B) or H1N1-infected vector control cells \pm SD (C).

(D) Western blot analysis of antiviral gene expression in basal (mock) or in H1N1-infected conditions. Vector control and *CIC* KO2s were infected with H1N1 (MOI = 5), and cell lysates were analyzed at 16 hpi.

(E) IFIT1 and MxA reporter activity upon ectopic expression of *CIC* and *ATXN1*. Firefly luciferase reporters under the control of *IFIT1* or *MxA* promoters were transfected in the presence or in the absence of RIG-I-2CARD, *CIC*, and *ATXN1*, and luciferase activity was measured at 48 hr post-transfection. Data are represented as percent luciferase activity relative to GFP + RIG-I-2CARD-transfected control \pm SD.

(F) Western blot analysis of *CIC* degradation upon H1N1 infection. Vector control and *CIC* KO2s were infected with H1N1 (MOI=3), and cell lysates were analyzed at the indicated times.

(G) qRT-PCR analysis of *CIC* downregulation upon H1N1 infection. WT A549s were infected with H1N1 (MOI = 5), and *CIC* mRNA levels were measured at 16 hpi. Data are represented as the fold expression relative to uninfected (mock) WT A549s \pm SD. For (D) and (F), *Ku* levels are shown as loading controls. * $p < 0.05$; ns, non-significant.

Data are representative of at least three independent experiments.

See also Figure S5.

Table 1

Enrichment of Selected Top Hits for Validation

Hits	Prelim Rd5	Rd2	Rd5
SLC35A1	1.2072×10^{-5}	2.37×10^{-7}	2.37×10^{-7}
GDF11	0.0045223	0.00038276	0.00032784
IRX3	0.0077903	0.015112	0.00081498
C2CD4C	0.0020496	0.0025642	0.0017149
TRIM23	0.015962	0.025194	0.001811
PIGN	0.0028786	0.0015024	0.0021415
ACADSB	0.011031	0.0023905	0.0021926
GRAMD2	0.021846	0.0059108	0.0028634
CIC	0.0053707	0.31911	0.0053541
JAK2	0.056382	0.16907	0.0063662
PIAS3	0.047231	0.33451	0.0077567

Of the 63 overlapping hits identified in the preliminary consecutive screen (Prelim Rd5) and Rd2 and Rd5 of the sequential screen, 11 genes involved in various biological processes were selected for further validation. p values for enrichment in the various rounds are shown.